



Design and mechanism of iron catalyzed carbon–carbon bond cleavage and N-oxidation processes of hazardous dyes for selective synthesis of nitroarenes and aminoarene-carboxylic acids

Rajenahally V. Jagadeesh*, T. Kiran, Pundlik R. Bhagat*, S. Senthil Kumar, P. Nithya, F. Nawaz Khan, A. Sivakumar

Division of Organic Chemistry, School of Advanced Sciences, Vellore Institute of Technology University, Vellore 632014, India

ARTICLE INFO

Article history:

Received 12 November 2010

Received in revised form 17 January 2011

Accepted 3 February 2011

Available online 3 March 2011

Keywords:

Iron catalyst

Oxidative degradation process

Hazardous dyes

Reaction mechanism

ABSTRACT

An efficient iron catalyzed oxidative degradation process has been developed for selective conversion of environmentally hazardous azo and indigo dyes into nitroarenes and aminoarene-carboxylic acids (anthranilic acids) respectively, using polymer supported tribromide reagent at an alkaline pH. The *in situ* generated and the isolated (defined) chloro-iron(II)-terpyridine–pyridine carboxylate [Fe(tpy)(pic)Cl] catalyst system has been developed and its catalytic function was invented for the degradation process. The different nitrogenous and oxygen ligands have been screened out for the development of best catalyst system, and eventually we explored pyridine 2-carboxylic acid and terpyridine ligands together, were found to be the best. Notably, the *in situ* generated and the defined catalyst systems have found to be more effective with similar catalytic activities towards the oxidative degradation of both the dyes. As a result, the whole oxidative degradation process has been carried out with Fe(tpy)(pic)Cl catalyst system and the general process utilizes the efficient catalytic method for the selective oxidation of –N=N– and –C=C– bonds of azo and indigo dyes respectively. The detailed catalysis, mechanistic and kinetic investigations have been made for the reactions. Interestingly, both the dyes proceed with a common oxidative degradation mechanism under identical kinetic patterns. A common oxidative degradation mechanism which operates in both the dyes has been proposed and an identical related kinetic model was designed. The main interesting aspect of the present work pertains to the catalytic conversion of environmentally hazardous compounds into useful molecules; such are anthranilic acids and nitrobenzenes. Other special aspect related to catalytic activity of iron and potentially, iron catalyst accelerates the reaction rates with 15–20-fold faster. The reactions were also carried out with different polymer supported trihalide and inter-halide reagents. Notably, trichloride and inter-halide reagents were found to be more reactive. The catalytic method developed for the degradation process was found to be very efficient and the involvement of cost-effective reagents makes the reaction simple, and can be conveniently scalable to industrial/technological operations with suitable modifications.

© 2011 Elsevier B.V. All rights reserved.

1. Introduction

Azo (**1**) and indigo (**2**) dyes (Fig. 1) are the two classes of dyes and are used extensively for dyeing cotton, textile and fabrics. Azo dyes have –N=N– moiety, extremely versatile colorants constitute about 50% of dyes produced [1]. About 30% of the initial azo dyes applied remain unfixed, which causes the poor exhaustion to end up in hazardous effluents [2]. Indigo is the vat dye and commonly used for the manufacture of denim. Around 5–20% of indigo dyes also remain unfixed [3] and the unfixed dyes form

effluent, which causes environmental hazardous. No doubt, these dyes are useful synthetic or natural compounds and used for dyeing purposes as well as analytical reagents for estimation purposes. However, these dyes form hazardous effluents in other hand and which affect both aerobic and aquatic living systems. Dyes are synthetic in nature with a complex chemical structure; persist in the natural biotic environment. Some of these dyes are carcinogens and mutagens, and some dyes also cause harm to the flora and fauna in the natural environment. Dyes in water create aesthetic problems, leading to the limited possible use of water and become toxic to microorganisms [4]. Due to the environmental hazardous effect, the degradation of dyes has considerable attention and seeks development of efficient degradation protocols. Nevertheless, to the best of our knowledge, some processes have been developed for the

* Corresponding authors. Tel.: +91 9731989352.

E-mail address: rvjdeesh@gmail.com (R.V. Jagadeesh).

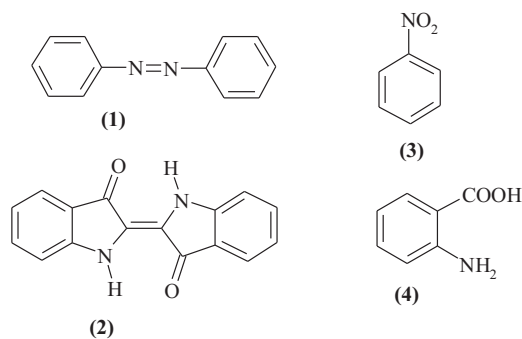


Fig. 1. Azo dye, indigo dye, nitrobenzene and anthranilic acid.

degradation and decolorization of dyes [5–16]. Modern chemical methods include TiO_2 -mediated photo degradation [5–8], Fenton systems [9] and transition metal catalysts in combination with wide range of oxidizing agents [10–16]. However, there is a still need of developing efficient degradation process by introducing cost-effective catalysts and stable reagent systems. For this reason, we are describing the detailed investigations of the use of Fe-catalyst for the oxidative degradation of azo and indigo dyes with polymer supported Br_3^- oxidant. The most important aspect in the present research is the synthesis of useful molecules, nitrobenzenes (3) and anthranilic acids (4) from the hazardous azo and indigo dyes.

More specialized applications of nitrobenzenes include the use as a precursor to rubber chemicals, pesticides, dyes, explosives, and pharmaceuticals. Presumably, nitrobenzenes have been used in the production of analgesic, paracetamol, and as an inexpensive perfume for soaps. Generally, the nitrobenzenes were synthesized either by the typical nitration of benzenes or oxidation of anilines. Other than these, there were not much attempts made towards the synthesis of nitrobenzenes with alternative methods. Other interesting molecules, anthranilic acids possess versatile properties and constitutes many pharmaceutical, medicinal and synthetic applications [17,18]. Based on the various applications and uses of nitrobenzenes and anthranilic acids, the synthesis of these molecules comes out to be an important and noteworthy research.

Oxidation reactions using platinum group metal [19–22] catalysts constitute probably one of the most important developments in synthetic and oxidation chemistry from last few decades. However, platinum group metal complexes are expensive and usually air and moisture sensitive. The limited availability of these metals and as a consequence thereof the high price as well as the significant toxicity makes it desirable to search for more economical and environmental friendly alternatives. A possible solution of this problem could be the increasing utilization of catalysts based on transition metals, such as iron, copper, chromium, and manganese [23–25]. Especially iron offers significant advantages compared to precious metals, since it is the second most abundant metal in the earth crust (4.7%). Various iron salts and iron complexes are commercially accessible on large scale or easy to synthesize. Furthermore, iron compounds are relatively non-toxic and cheaper. However, most of the known catalytic reactions with iron are limited and the use of iron as catalyst is so far not much developed when compared to precious metals. Based on the background of cost effectiveness and stability of iron source, we have developed three component catalyst system (5) based on FeCl_2 , pyridine carboxylic acid (L_1 ; pic) and terpyridine (L_2 ; tpy) ligands (Fig. 2) for the selective degradation of dyes.

Functionalized polymers have been used to promote a wide range of organic transformations and the current status on the uses of polymer supported reagents for oxidation and synthetic

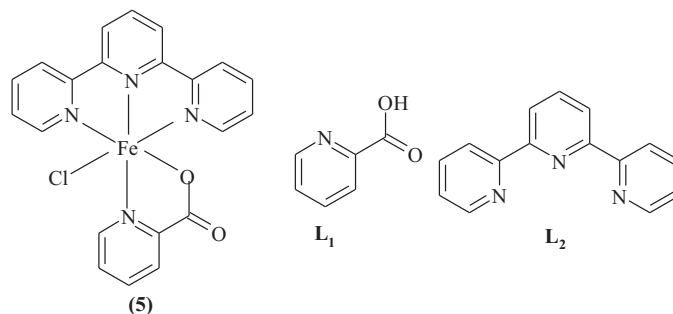


Fig. 2. Iron catalyst $[\text{Fe}(\text{II})(\text{tpy})(\text{pic})\text{Cl}]$ and nitrogen ligands.

purposes have been examined in the fine chemistry [26,27]. Applications of polymer supported reagents in organic synthesis have grown over the years due to convenient handling and easy work up procedures [26,27]. Polymer supported reagents have been widely used in organic synthesis due to their numerous advantages including ease of separation of products, less amount of reagent is sufficient to bring out the reaction, reactions are environmentally benign and easy to work-up. The numerous applications of polymer supported reagents prompted to propose polymer supported Amberlyst A 26 Br_3^- resin (Fig. 3) resin (6) as the oxidant for the degradation process of dyes. Polymer bound tribromide reagents are more suitable and safer than molecular halogens because these are solids and hence easy to handle, and owing to their stability, selectivity and excellent product yields. Based on the reaction conditions the tribromide reagents act as both oxidizing and brominating agents [28–30]. The bromination process with these reagents probably takes place in drastic conditions at elevated temperatures. But these reagents were effective oxidants in mild conditions especially, in acidic or alkaline medium. Interestingly, under alkaline condition the tribromide reagent was functioned as oxidant in the present study rather than the brominating agent.

The wide range of hazardous nature of dyes, usefulness of iron catalyst in organic reactions, versatile applications of polymer supported reagents, and industrial as well as pharmaceutical applications of nitrobenzenes and anthranilic acids instigate us to develop a protocol for the oxidative degradation of azo and indigo dyes with an objective of studying reaction mechanism including kinetic interpretations. As a consequence, we reported herein a new, simple and cost-effective method for the oxidative degradation of dyes using iron catalyst and Br_3^- reagent (Scheme 1).

2. Experimental

2.1. General

Unless specified, all chemicals are commercially available and used as received without further purification. $\text{Fe}(\text{tpy})(\text{pic})\text{Cl}$ was prepared. Qualitative and quantitative analysis of reaction products were done on 17A Shimadzu gas chromatograph with a QP-5050A Shimadzu mass spectrometer. UV–vis spectroscopic and kinetic measurements were performed with a Shimadzu UV-1601 spectrophotometer.

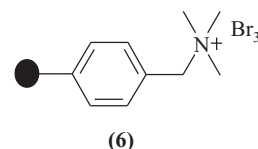
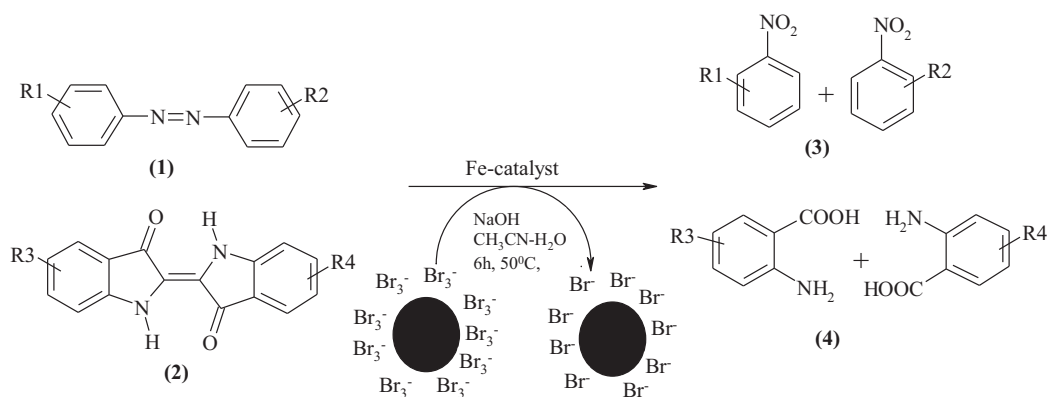


Fig. 3. Amberlyst A 26 tribromide resin.



Scheme 1. Iron catalyzed oxidative degradation process of azo and indigo dyes.

2.2. Capacity of Br₃⁻ resin

The capacity of tribromide resin was achieved using L-ascorbic acid. The chemical removal of Br₃⁻ was achieved by reducing Br₃⁻ by feeding stoichiometric excess of L-ascorbic acid (0.1 M) in 0.10 M HCl slowly through the resin bed until all traces of Br₃⁻ were removed. The determination of ascorbic acid amount in feed and in the effluent was done by iodometric titrations. The amount of L-ascorbic acid consumed for reducing (difference in the amount of ascorbic acid in feed and in effluent) Br₃⁻ gave the capacity of Br₃⁻ resin. The capacity of the resin was found to be 1 mmol/g.

2.3. Preparation of iron catalyst [Fe(tpy)(pic)Cl] (catalyst 5)

The iron catalyst was prepared using FeCl₂, 2,2',6',2''-terpyridine (tpy) and 2-pyridine carboxylic acid (pic) in aqueous methanol under argon. FeCl₂ (127 mg, 1 mmol) and 2,2',6',2''-terpyridine (233 mg, 1 mmol) were dissolved in MeOH (30 mL) at room temperature under argon. 2-Pyridine carboxylic acid (123 mg, 1 mmol) and NaOH (40 mg, 1 mmol) were dissolved in H₂O (20 mL) by stirring to get sodium 2-pyridine carboxylate and to this 40 mL MeOH was added. This solution was purged with argon for 20 min and then added drop wise to the reaction mixture using cannula. The whole reaction mixture was heated at 50 °C for 2 h under stirred condition in argon. After, the reaction mixture was cooled to room temperature, CH₂Cl₂ (25 mL) and H₂O (25 mL) were added. The organic layer was separated and the aqueous layer was extracted with CH₂Cl₂ thoroughly. The combined organic layer was dried over MgSO₄, filtered and the solvent was removed under reduced pressure followed by drying at high vacuum. The yield of the product was found to be around 70%. The product was not soluble enough to give satisfactory ¹H and ¹³C spectra. UV-vis (CH₂Cl₂, λ_{max}/nm, log e) 350 (4.48), 412 (3.81), 551 (3.56). HRMS Calc. for (C₂₁H₁₅ClN₄O₂Fe) m/z: 446.677. Found: 446.559. Elemental analysis: Calculated (%) C = 56.47, H = 3.38, N = 12.54, Fe = 12.50, Cl = 7.94. Found: C = 56.87, H = 3.39, N = 12.64, Fe = 12.56, Cl = 8.01.

2.4. Procedure for oxidative degradation process with in situ generated catalyst

In 50 mL round bottomed flask, FeCl₂ (0.01 mmol), terpyridine (0.01 mmol) were dissolved in 14 mL 1:1 acetonitrile–water. To this solution, sodium 2-pyridine carboxylate (0.01 mmol) in 2 mL water–acetonitrile was added and stirred for 1 h at 50 °C. Then, corresponding dye (0.5 mmol) in 2 mL 1:1 acetonitrile–water, Amberlyst A Br₃⁻ resin (2 g) were added followed by the addition of NaOH (0.5 mmol) in 2 mL water–acetonitrile. The whole reaction mixture was stirred for 26 h at 70 °C. After, the reaction products

were cooled to room temperature, slowly neutralized with acid and the solid oxidant was filtered off. Dodecanese (100 μL) was added as an internal standard, and samples of the mixtures were directly subjected to GC and MS analysis. The qualitative and quantities estimations were made using GC and mass spectral analysis and also by comparing with authentic samples.

2.5. Procedure for the oxidative degradation process with defined (isolated) catalyst (catalyst 5)

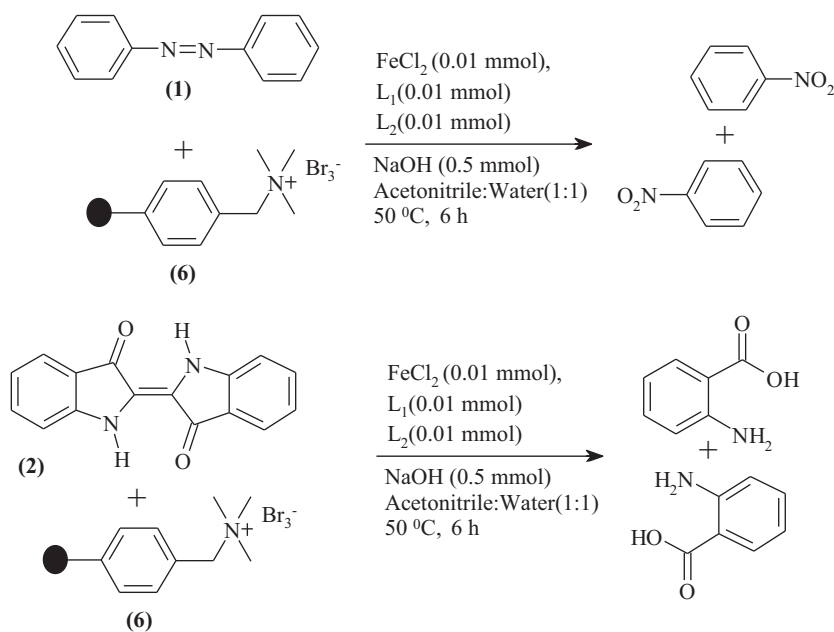
Solution of catalyst (1) (0.01 mmol) dissolved in 1:1 acetonitrile–water (16 mL) was treated in ultrasound for 20 min. Then, corresponding dye (0.5 mmol) in 4 mL 1:1 acetonitrile–water, Br₃⁻ resins (2 g) and 0.5 mmol NaOH in 2 mL 1:1 acetonitrile–water were added, and the reaction mixture was allowed to proceed under stirred condition for 26 h at 70 °C. After, the reaction products were cooled to room temperature, slowly neutralized with acid and the solid oxidant was filtered off. Dodecanese (100 μL) was added as an internal standard, and samples of the mixtures were directly subjected to GC and MS analysis. The qualitative and quantities estimations were made using GC and mass spectral analysis when compared with authentic sample.

2.6. Recycling of Br₃⁻ resin

Successfully, the tribromide resin was recycled and was used 5 times without much significant loss of resin chemical composition of the polymer matrix by retaining original resin capacity. After completion of reaction the resin resides in the form of Br⁻. After the reaction the resin was filtered, washed with acetonitrile and dried in air and then under vacuum. The dried Br⁻ form of resin was treated with NaBr solution followed by excess of bromine in acetonitrile. The tribromide resin was air and vacuum dried and then used without any further purification.

2.7. Procedure for spectrophotometric kinetic studies

The detailed kinetic experiments were made with respect to conversion of azobenzene and indigo in alkaline acetonitrile–water (1:1) as model reactions. The reactions were carried out under pseudo first-order conditions with a known excess of [Br₃⁻] over [dye] spectrophotometrically at 70 °C. All reactants were dissolved in aqueous acetonitrile (1:1). The solution of dye (azobenzene or indigo), catalyst, NaOH and acetonitrile–water (to keep constant volume) were thermostated at 70 °C under stirred condition. The known excess of oxidant (in acetonitrile–water) over dye was also thermostated at 70 °C under stirred condition. After attaining the equilibrium temperature, the oxidant was added to the reaction



L_1 =2-Pyridinecarboxylate (pic); L_2 =Different nitrogen ligands

Scheme 2. *In situ* generated iron catalyzed oxidative degradation of dyes.

mixture and continued stirring at 70 °C. The absorbance of reaction mixture was measured in different intervals of time at 319 nm (λ_{max}) for azobenzene and 602 nm (λ_{max}) for indigo up to three half-lives. The absorbance readings at $t=0$ and $t=t$ are D_0 and D_t . The pseudo first-order rate constants (k') were evaluated from the plots of $\log D_0/D_t$ vs time.

3. Results and discussion

The initial oxidation degradation processes were carried out with azobenzene and indigo at 50 °C as model compounds. The reactions were studied in various solvents (acetonitrile, THF, ethanol, dioxane and acetonitrile–water (1:1) mixture). The mixture of acetonitrile–water (1:1) is found to be the best solvent system, perhaps due to good dielectric constant. The reactions were found to be highly dependent on pH of the system. To evaluate the effect of pH, the reactions were carried out under similar experimental conditions at different pH's using NaOH. At neutral pH, the oxidative degradation reactions were found to be very slow, however the reaction rates increase with increasing in pH (addition of NaOH). Due to increase of reaction rate in the presence of NaOH, the reactions were carried out at alkaline pH.

3.1. Oxidative degradation process in presence of *in situ* generated catalyst and screening of ligands

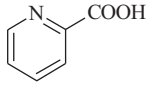
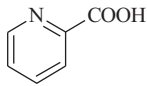
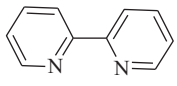
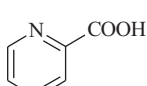
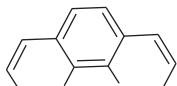
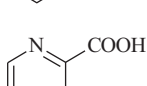

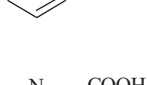
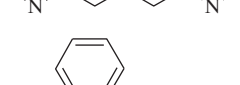
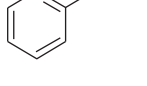
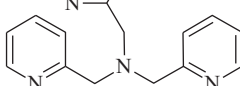
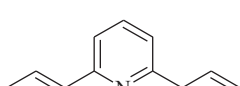
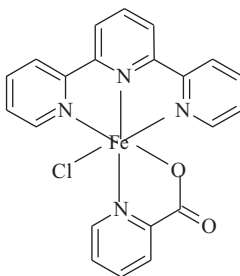
Initially, the oxidative degradation of azobenzene and indigo was carried out with Br_3^- in aqueous alkaline acetonitrile medium in the presence of FeCl_2 . In the presence of FeCl_2 alone we could not be able to get appreciable oxidative conversion (50%). These results instigate us to search for good ligands for FeCl_2 to get facile conversion rates. Generally, catalytic efficiency of metal catalysts increases in the presence of ligands due to increased electron density of catalyst system. Notably, nitrogen, oxygen and phosphorus ligands are the better choice, which enhance the catalytic properties of metals. An account of above facts, our study tuned

towards the use of aforementioned ligands. Interestingly, the oxidation conversion (65%) increased in the presence of added ligand, 2-pyridine carboxylic acid (pic; L_1) as *in situ* generated catalyst system. But notably, the conversion rate increases in the presence of additional nitrogen ligands (L_2). Then, screening for the best nitrogen ligand was sought in the presence of L_1 and to our delight, terpyridine (tpy; L_2) ligand is found to be the best and efficient along with L_1 . The conversion rate was increased to 100% with an *in situ* generated catalyst system in the presence of L_1 (pic) and terpyridine (tpy; L_2) ligands (Scheme 2). Importantly, the conversion rate could not be achieved efficiently in the presence of single ligand either with L_1 or L_2 alone. By all these experimental results it was concluded that the *in situ* generated FeCl -terpyridine–pyridine carboxylate complex was found to be the best catalyst system for the degradation process. These results are tabulated in Table 1. The reactions were also carried out with different iron precursors such as FeCl_2 , $\text{Fe}(\text{OAc})_2$, $\text{Fe}(\text{NO}_3)_2$ and FeSO_4 under the prevailing experimental condition. However, FeCl_2 was found to be better iron precursor compared to other ones.

3.2. Oxidative degradation process in presence of defined catalyst system (catalyst 5)

In the presence of an *in situ* generated catalyst, oxidative degradation of dyes was achieved remarkably with full conversion. It was thought interesting to prepare and isolate the defined FeCl -terpyridine–pyridine carboxylate (catalyst 5) (Scheme 3) catalyst and to study its catalytic activity for the degradation processes. Thus, the defined chloro-iron-terpyridine–pyridine-2-carboxylate complex $[\text{Fe}(\text{II})(\text{tpy})(\text{pic})\text{Cl}]$ (catalyst 5) was prepared and obviously, in the presence of defined catalyst the dyes under go oxidative degradation with full conversion (100%). Once the degradation conversion was found 100%, then the oxidative degradation of different dyes were carried out in aqueous alkaline acetonitrile medium with Br_3^- oxidant in the presence of catalyst 5 (Scheme 4). These results were summarized in Tables 2 and 3.

Table 1
Ligand screening and *in situ* generated catalysis process for the oxidative degradation of dyes^a.

Entry	Iron precursor	Ligand (L ₁)	Ligand (L ₂)	Conversion (%)	
				Azo benzene	Indigo
1	FeCl ₂	–	–	50	50
2	FeSO ₄	–	–	25	21
3	Fe(NO ₃) ₂	–	–	22	19
4	Fe(OAc) ₂	–	–	35	35
5	FeCl ₂		–	65	63
6	FeCl ₂			75	73
7	FeCl ₂			80	74
8	FeCl ₂			88	86
9	FeCl ₂			85	82
10	FeCl ₂			100	100
11	FeCl ₂	–		64	64
12 ^b	FeCl ₂	Catalyst 5		100	100

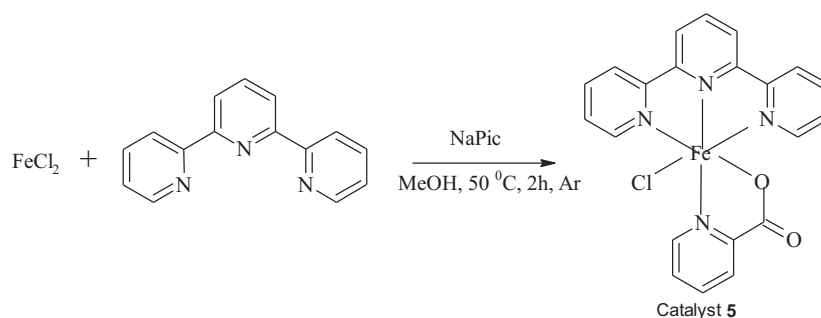
^a Dye = 0.5 mmol, FeCl₂ = 0.01 mmol, L₁ = 0.01 mmol, and NaOH = 0.5 mmol.

^b Dye = 0.5 mmol, catalyst **5** = 0.01 mmol, NaOH = 0.5 mmol, and temperature = 70 °C.

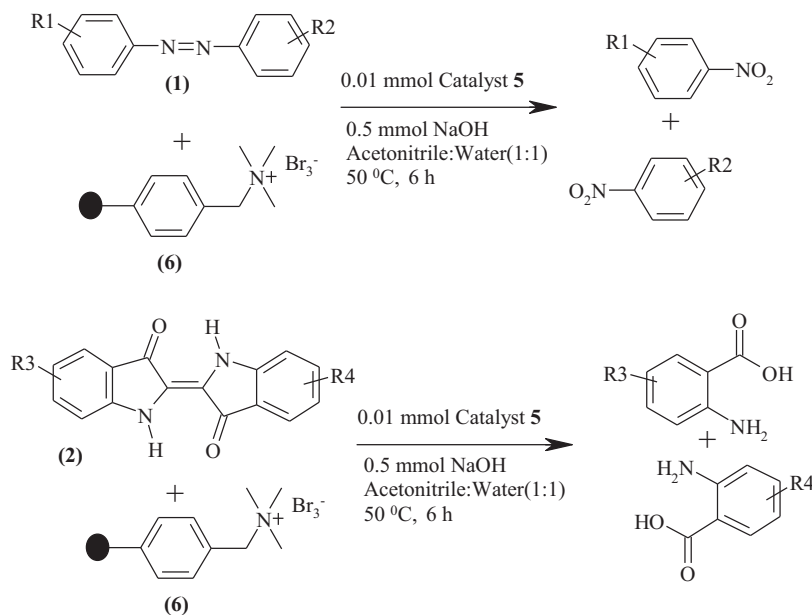
3.3. Kinetics of oxidative degradation process

The oxidative degradation kinetics of azobenzene and indigo as model compounds by Br₃[−] has been investigated in the presence of NaOH using catalyst **5** at 70 °C. More interestingly, the similar oxidative degradation kinetic behavior is observed for both azobenzene and indigo under identical experimental conditions. Obviously, all the dyes studied underwent degradation with similar mechanism implying by identical kinetic patterns. It is interesting to note that the azo dye underwent with faster conversion rate than the indigo dye.

With [Br₃[−]] in excess, at constant [NaOH], [Iron] and temperature, plots of log[Dye] vs time were linear ($R^2 > 0.9890$) indicating first-order dependence of rate on [Dye]. The values of pseudo first-order rate constants (k') are given in Table 4. Further, the values of k' were unaffected with the addition of [Dye], confirming first-order dependence of rate on [Dye]. Under the similar experimental conditions, an increase in [Br₃[−]] led to increase in the reaction rates (Table 4). Plots of log k' vs log[Br₃[−]] were linear (Fig. 4; $R^2 > 0.9899$) with unit slopes, show first-order dependence of rate on [Br₃[−]]. Further, plots of k' vs [Br₃[−]] were linear ($R^2 > 0.9900$) passing through the origin, confirming the first-order dependence of rate with [Br₃[−]]. The rate of the reaction increases with increase



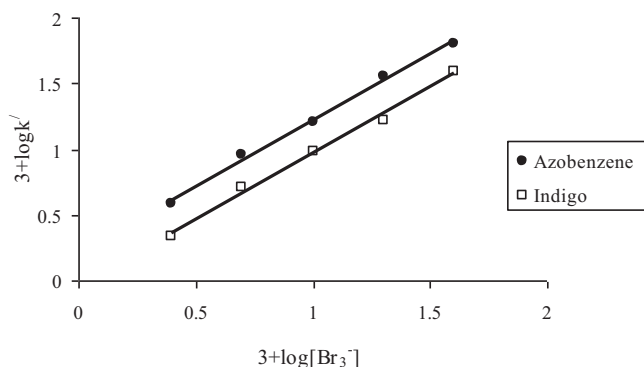
Scheme 3. Preparation of [Fe(tpy)(pic)Cl].



Scheme 4. Defined iron catalyzed oxidative degradation of dyes.

in [NaOH] (Table 4) and plots of $\log k'$ vs $\log[\text{NaOH}]$ were linear (Fig. 5; $r > 0.9901$) with positive slopes (0.45–0.55), indicating fractional-order dependence of rate on [NaOH]. The rate of the reaction was also increased with increasing [Iron] (catalyst 5) (Table 4) and the plots of $\log k'$ vs $\log[\text{Iron}]$ were linear (Fig. 5; $r > 0.9911$) with slopes equal to one indicating a first-order dependence of rate on [Iron].

Rate studies were carried out in H_2O – MeOH mixtures having different compositions (0–30%, v/v), thereby varying the dielectric constant of the solvent medium. The rate was found to decrease with increase in MeOH content (decrease in dielec-

Fig. 4. Plots of $\log k'$ vs $\log[\text{Br}_3^-]$.

tric constant) (Table 5) and plots of $\log k'$ vs $1/D$ were linear ($r > 0.9901$) with negative slopes. Rate studies in D_2O medium for azobenzene and indigo revealed that $k'(\text{H}_2\text{O}) = 16.0 \times 10^{-3} \text{ s}^{-1}$ and $9.55 \times 10^{-3} \text{ s}^{-1}$, and $k'(\text{D}_2\text{O}) = 21.6 \times 10^{-3} \text{ s}^{-1}$ and $13.5 \times 10^{-3} \text{ s}^{-1}$

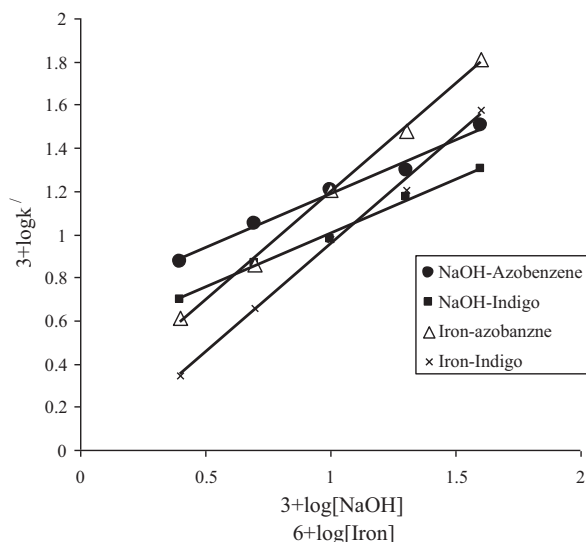
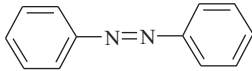
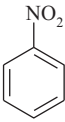
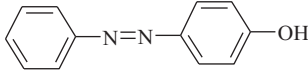

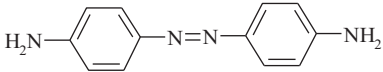

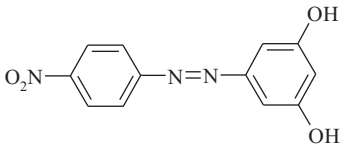
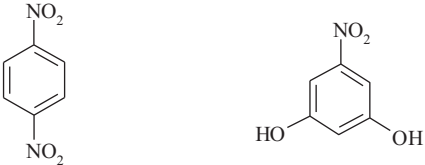
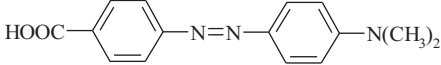

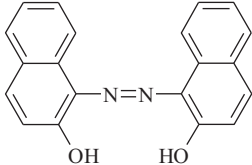
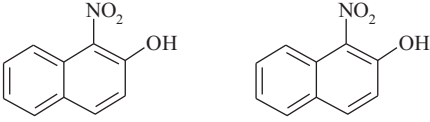
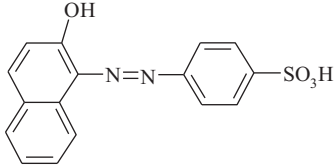
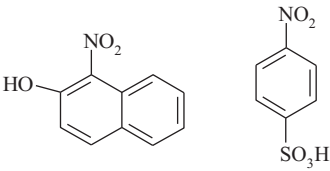
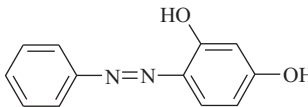

Fig. 5. Plots of $\log k'$ vs $\log[\text{NaOH}]$ and $\log k'$ vs $\log[\text{Iron}]$.

Table 2
Oxidative degradation of azo dyes with catalyst **5**^a.

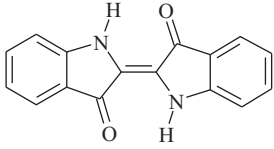
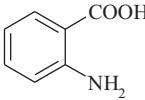
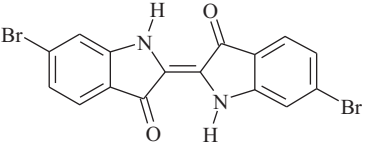
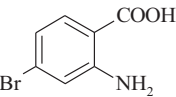
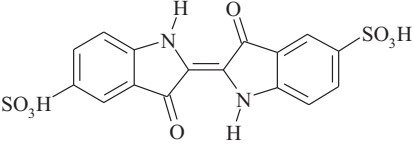
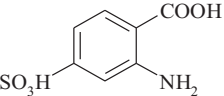
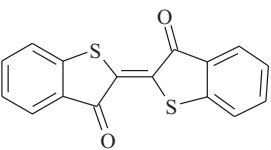
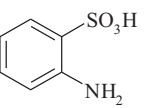
Entry	Azo dye	Product (s)	Conversion (%)	Yield (%)
1			100	90
2			100	90
3			100	90
4			100	85
5			100	85
6			>99	91
7			>99	89
8			>99	91

^a Dye = 0.5 mmol, catalyst **5** = 0.01 mmol, NaOH = 0.5 mmol, and temperature = 70 °C.

respectively. The formal solvent isotope effect, $k'(H_2O)/k'(D_2O)$ was found to be 0.74 and 0.70 for these two compounds. Solvent isotope studies were made by using H₂O–D₂O mixtures for azobenzene and indigo (Table 5). The effect of the temperature on the reaction rate was studied by performing the kinetic experiments at various temperatures (323–353 K), keeping other experimental conditions constant. From the linear Arrhenius plots of $\log k'$ vs $1/T$ (Fig. 6; $R^2 > 0.9911$), the values of

activation parameters (E_a , ΔH^\ddagger , ΔG^\ddagger , ΔS^\ddagger) for the overall reaction were evaluated. These data are summarized in Table 6. The effects of ionic strength (NaClO₄; I) of the medium, NaBr, NaCl and benzyltrimethylammonium ion on the rate were studied. At experimental conditions, the addition of NaClO₄, benzyltrimethylammonium ion did not affect the rate of the reaction, but the reaction rates were found to be slightly decreased with increase in [NaBr] and [NaCl].

Table 3
Oxidative degradation of indigo dyes with catalyst **5**^a.

Entry	Indigo dye	Product	Conversion (%)	Yield (%)
1			100	89
2			>99	88
3			>99	95
4 ^b			100	90

^a Dye = 0.5 mmol, catalyst **5** = 0.01 mmol, NaOH = 0.5 mmol, and temperature = 70 °C.^b Product in this case is aminobenzenesulfonic acid.**Table 4**
Effect of varying reactants, NaOH and iron concentrations on the reaction rate at 343 K.

10 ³ [Dye] (mol dm ⁻³)	10 ² [Br ₃ ⁻] (mol dm ⁻³)	10 ² NaOH (mol dm ⁻³)	10 ⁵ [Catalyst 5] (mol dm ⁻³)	10 ³ k' (s ⁻¹)	
				Azobenzene	Indigo
0.25	1.0	1.0	1.0	16.1	9.45
0.5	1.0	1.0	1.0	15.8	9.60
1.0	1.0	1.0	1.0	16.0	9.55
2.0	1.0	1.0	1.0	16.2	9.50
4.0	1.0	1.0	1.0	15.9	9.48
1.0	0.25	1.0	1.0	3.86	2.14
1.0	0.50	1.0	1.0	8.00	5.10
1.0	1.0	1.0	1.0	16.0	9.55
1.0	2.0	1.0	1.0	36.1	16.5
1.0	4.0	1.0	1.0	63.1	39.0
1.0	1.0	0.25	1.0	7.50	5.01
1.0	1.0	0.50	1.0	11.2	7.34
1.0	1.0	1.0	1.0	16.0	9.55
1.0	1.0	2.0	1.0	19.8	14.8
1.0	1.0	4.0	1.0	32.0	20.0
1.0	1.0	1.0	0.25	4.12	2.22
1.0	1.0	1.0	0.5	7.32	4.52
1.0	1.0	1.0	1.0	16.0	9.55
1.0	1.0	1.0	2.0	30.0	16.1
1.0	1.0	1.0	4.0	65.0	37.0

3.4. Reactive species of oxidant and catalyst

Polymer supported Br₃⁻ resin is an ionic compound and exists as polymer bound benzyltrimethylammonium cation and free tribromide anion in solution during stirring process as indicated in the following equilibrium (Eq. (1)).



(1)

Tribromide ion undergoes dissociation [31] to furnish bromine and bromide ion, and the dissociation constant values have been reported [31].



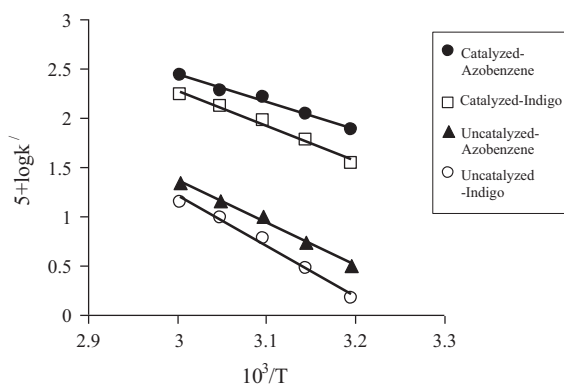
The generated Br⁻ combines with polymer bound benzyltrimethylammonium cation to form benzyltrimethylammonium bromide resin. The kinetic studies indicate that the reaction

Table 5
Effect of varying dielectric constant and solvent isotope on the reaction rate at 343 K.

% [MeOH] (v/v)	<i>D</i>	10 ³ <i>k'</i> (s ⁻¹)	
		Azobenzene	Indigo
0.0	76.73	16.0	9.55
10.0	72.37	12.5	8.32
20.0	67.48	11.1	6.45
30.0	62.71	8.98	5.00

Atom fraction of deuterium (<i>n</i>)	10 ³ <i>k'_n</i> (s ⁻¹)		<i>(k'_o/k'_n)</i> ^{1/2}	
	Azobenzene	Indigo	Azobenzene	Indigo
0.00	16.0	9.55	1.0	1.0
0.25	17.3	10.8	0.96	0.94
0.50	18.9	11.7	0.92	0.90
0.75	20.2	12.6	0.89	0.87
0.95	21.6	13.5	0.86	0.84

[Dye]₀ = 1.0 × 10⁻³ mol dm⁻³; [Br₃⁻]₀ = 1.0 × 10⁻² mol dm⁻³;
[NaOH] = 1.0 × 10⁻² mol dm⁻³; [catalyst **5**] = 1.0 × 10⁻⁵ mol dm⁻³.

**Fig. 6.** log *k'* vs 1/*T*.

rate increases with increasing OH⁻. Under increasing reaction rate in the presence of OH⁻, Br₂ forms BrOH species and this species, BrOH has been postulated as the reactive oxidizing species in the present study under prevailing experimental conditions.



Under the experimental conditions, [OH⁻] » [catalyst **5**] and the fact that [OH⁻] increases the rate, catalyst **5** is mostly present as hydroxylated species and its formation is given in the following

Table 6
Temperature dependence, catalytic constants (*K_c*) and values of activation parameters.

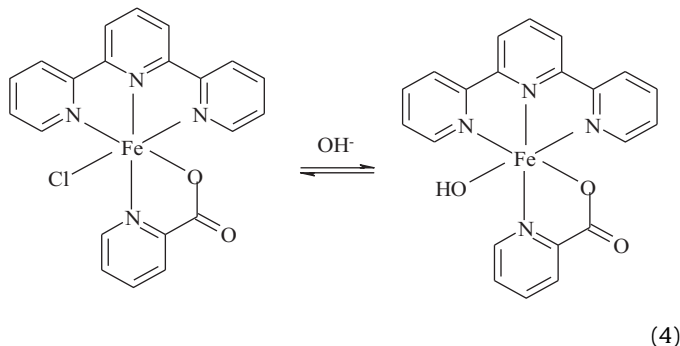
Temperature (K)	10 ³ <i>k'</i> (s ⁻¹)		<i>K_c</i>	
	Azobenzene	Indigo	Azobenzene	Indigo
333	7.50(0.32) ^b	3.51(0.15)	71.8	33.6
338	11.1(0.55)	6.01(0.32)	104	57.0
343	16.0(1.00)	9.55(0.60)	150	89.5
348	19.0(1.42)	13.0(0.96)	176	120
353	27.1(2.21)	17.1(1.20)	248	156
<i>E_a</i> (kJ mol ⁻¹)	50.2(76.6)	63.6(92.0)	64.0	81.8
ΔH^\ddagger (kJ mol ⁻¹)	47.5(73.9)	61.0(89.0)	61.4	79.2
ΔG^\ddagger (kJ mol ⁻¹)	93.0(102)	92.5(101)	77.4	75.7.0
ΔS^\ddagger (J K ⁻¹ mol ⁻¹)	-138(-85.6)	-99.6(-41.8)	-44.0	-8.28

Values in parentheses refer in the absence of catalyst **5**.

^a [Dye]₀ = 1.0 × 10⁻³ mol dm⁻³; [Br₃⁻]₀ = 1.0 × 10⁻² mol dm⁻³;
[NaOH] = 1.0 × 10⁻² mol dm⁻³; [catalyst **5**] = 1.0 × 10⁻⁵ mol dm⁻³.

^b Experimental conditions are same as 'a' without iron catalyst **5**.

equilibrium:



The hydroxylated species of catalyst **5** has been postulated as the reactive species in alkaline medium for the oxidative conversion of dyes.

3.5. Intermediate complex existence between dye and iron catalyst

UV–vis spectral studies have been made for the evidence to show the existence of intermediate complex between dye (azobenzene or indigo) and catalyst **5**. UV–vis spectral studies indicate the intermediate complex formation took place between azobenzene and catalyst **5** in which a shift of azobenzene from 319 nm to 332 nm was observed in the presence catalyst **5**.

The complex formation between dye (azobenzene) and catalyst **5** was given by the following equilibrium (Eq. (5)):

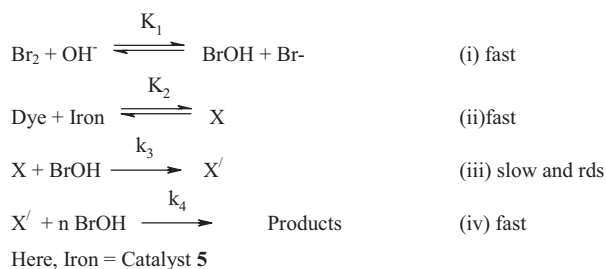


Here, M and MS_{*n*} are two metal species (catalyst **5** species) with different extinction coefficients. For the above equilibrium (5), the following [32] relation has been derived (Eq. (6)):

$$\frac{1}{\Delta A} = \frac{1}{[S]^n} \left\{ \frac{1}{\Delta E[M_{\text{Total}}]K} \right\} + \frac{1}{\Delta E[M_{\text{Total}}]} \quad (6)$$

where *K* is the formation constant of the complex, [S] is the concentration of Dye, ΔE is the difference in extinction coefficient between two metal species, [M]_{Total} is the total concentration of metal species and ΔA is the absorbance difference between dye–iron mixture and iron alone. Eq. (6) is valid when [S] is much higher than [M]_{Total}. According to Eq. (6), a plot of 1/ ΔA vs 1/[S] or 1/[S]² should be linear with an intercept in case of 1:1 or 1:2 type of complex formation between M and S. The ratio of intercept to slope of this linear plot gives the value of formation constant, *K*.

The complex formation studies between azobenzene and catalyst **5** were made at 332 nm in order to evaluate stoichiometry of the intermediate formation. The absorbance of solutions containing series of azobenzene (0.25 × 10⁻³–4 × 10⁻³ mol dm⁻³) in the presence of NaOH (1 × 10⁻² mol dm⁻³) and iron (1.0 × 10⁻⁵ mol dm⁻³) were measured at 332 nm. The absorbance of catalyst **5** alone (1.0 × 10⁻⁵ mol dm⁻³) in NaOH (1 × 10⁻² mol dm⁻³) was also measured at 332. The difference of absorbance (with and without catalyst **5**) gave the differential absorbance, ΔA . A plot of 1/ ΔA vs 1/[azobenzene] was linear (*R*² = 0.9898) with an intercept suggests the formation of 1:1 complex between azobenzene–catalyst **5**. Further, the plot of log(1/ ΔA) vs log(1/[azobenzene]) was also linear (*R*² = 0.9871). From the slope and intercept of the plot 1/ ΔA vs 1/[azobenzene], the value of the formation constant, *K* of the complex was deduced and was found to be 8.6 × 10². The hypsochromic shift of 20 nm of indigo from 602 nm to 582 nm in the presence of iron catalyst clearly indicates the formation of intermediate complex between indigo and catalyst **5**. The similar studies as mentioned with azobenzene have been made with indigo and



Scheme 5. Proposed mechanistic scheme for the oxidative degradation of dyes.

catalyst **5** at 582 nm. The studies show that there is an existence of 1:1 complex also between indigo and catalyst **5** system and the formation constant was found to be 6.23×10^2 .

3.6. Oxidative degradation mechanism

The kinetic results clearly confirm BrOH and the hydroxylated species of catalyst **5** have been postulated as the reactive species of oxidant and catalyst, which took part in the reaction. The UV–vis studies show the interaction of catalyst with dye which took place with the formation of transient intermediate. The identical kinetic data for both azo and indigo dyes imply the fact that the similar mechanism is being operated for the oxidative degradation of all the dyes. Based on the above discussion and the observed kinetic results, the common general mechanistic scheme (Scheme 5) has been proposed for the iron catalyzed oxidative degradation of dyes by Br_3^- in the presence of alkali.

In Scheme 5, X and X' represent the intermediate species. The detailed mechanisms for the iron catalyzed oxidative conversion of dyes were postulated in Schemes 6 and 7.

The total effective contribution of $[\text{Br}_3^-]$ is given by

$$[\text{Br}_3^-] = \text{Br}_2 + \text{BrOH} \quad (7)$$

From step (i) of Scheme 5,

$$[\text{Br}_2] = \frac{[\text{BrOH}][\text{Br}^-]}{K_1[\text{OH}^-]} \quad (8)$$

By substituting for $[\text{Br}_2]$ from Eq. (8) into Eq. (7) and solving for $[\text{BrOH}]$ we get,

$$[\text{BrOH}] = \frac{K_1[\text{Br}_3^-]K_1[\text{OH}^-]}{[\text{Br}^-]K_1[\text{OH}^-]} \quad (9)$$

From slow and rate determining step (iv) of Scheme 5, rate of reaction is given by

$$\text{Rate} = k_3[\text{X}][\text{BrOH}] \quad (10)$$

From step (ii) of Scheme 5,

$$[\text{X}] = K_2[\text{Dye}][\text{Iron}] \quad (11)$$

On substituting for $[\text{BrOH}]$ and $[\text{X}]$ from Eqs. (9) and (11) respectively into Eq. (10), one obtains the kinetic model (12):

$$\text{Rate} = \frac{K_1 K_2 K_3 [\text{Dye}][\text{Br}_3^-][\text{Iron}][\text{OH}^-]}{[\text{Br}^-] + K_1[\text{OH}^-]} \quad (12)$$

Based on Scheme 5, the kinetic model (Eq. (12)) derived is consistent with all the experimental kinetic results, in which first-order reaction rate with respect to $[\text{Dye}]$, $[\text{Br}_3^-]$ and $[\text{Iron}]$, and a fractional order with $[\text{NaOH}]$. Thus, Scheme 5 and the kinetic model (12) are consistent with the observed experimental kinetic results.

The studies implicate that the nitrogenous ligand, terpyridine was found to be the best ligand system together with pyridine 2-carboxylic acid. This might be attributed to higher electron density

of terpyridine ligand, compared to other ligands. Due to rich electron density of terpyridine ligand, which forms an effective and highly stabilized complex with Fe, and thereby increases the catalytic activity of Fe. The catalytic reaction was initiated by the interaction of catalyst species with dyes forming an intermediate. The so formed Fe-dye intermediate in the presence of oxidant undergoes further reaction to yield dihydroxylated compounds (both in azo and indigo dyes) with the regeneration of catalyst. The dihydroxylated dyes undergo further oxidation to produce corresponding nitrosobenzenes in case of azo dyes and isatins in case of indigo dyes. These intermediate, nitrosobenzenes and isatins were identified by GC and MS data. In the presence of excess oxidant, the nitrosobenzenes and isatins undergo final oxidation to produce ultimate and desired products, nitrosobenzenes and anthranilic acids. The detailed mechanisms and oxidative degradation pathways for the conversion of dyes were presented in Schemes 6 and 7.

The proposed mechanism was further supported by the following studies.

3.7. Studies on dielectric permittivity effect

The decrease of reaction rate with the decrease in D (increase in MeOH content) of the medium supports the proposed mechanism. Amis and Jaffe [33] have derived the following relation:

$$\log k'_D = \log k' + \frac{Ze\mu}{2.303kTr^2D} \quad (13)$$

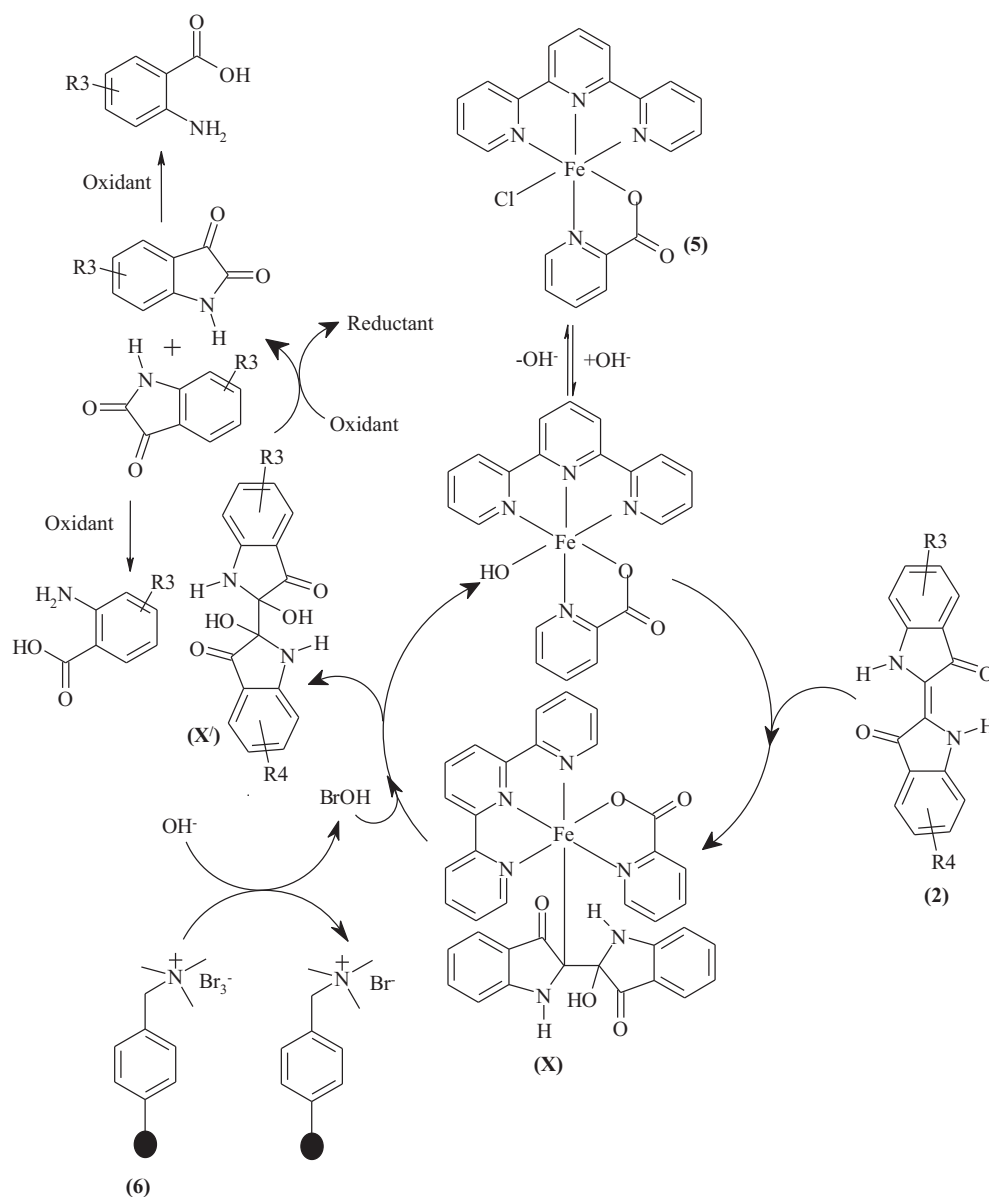
in which, k' is the rate constant in a medium of infinite dielectric constant and k'_D is the rate constant as function of dielectric constant D , Ze is the charge on the ion, μ is the dipole moment of the dipole, k is the Boltzmann constant, T is the absolute temperature and r is the distance of approach between the ion and dipole. Eq. (13) predicts a linear relation between $\log k'$ vs $1/D$ ($R^2 > 0.9901$). The slope of the line is negative for a reaction between a negative ion and a dipole or between two dipoles, while a positive slope is obtained for positive ion-dipole reactions. In the present investigations, plots of $\log k'$ vs $1/D$ were linear with negative slopes ($R^2 > 0.9901$) supporting the participation of two dipoles in the rate-determining step (rds).

3.8. Solvent isotope studies

It is an interesting fact that the reaction rates in D_2O medium are faster than that in H_2O . Since the OD^- is a stronger base than OH^- by a factor of 2–3, the solvent isotope effect of this magnitude is expected [34]. The observed inverse solvent isotope effect $k'(\text{D}_2\text{O})/k'(\text{H}_2\text{O})$ of 1.35 for azobenzene and 1.41 for indigo (Table 5) and the normal kinetic isotope effect $k'_{\text{OH}^-}/k'_{\text{OD}^-} < 1$ could counterbalance the solvent isotope effect, which can be attributed to the positive fractional-order dependence of rate on $[\text{OH}^-]$. The effect by factor 2–3 could have been expected when the reaction rate with respect to $[\text{OH}^-]$ would be unit order. But this was not expected due to the fractional orders with respect to $[\text{OH}^-]$. The solvent isotope studies in H_2O – D_2O mixtures could throw light on the nature of the transition state [35,36] and the dependence of rate constant k'_n on the atom fraction of deuterium (n) in a solvent mixture, is given [36] by Eq. (9):

$$k'_o/k'_n = \pi \left(\frac{\text{TS}}{1 - n + n\Phi_i} \right) / \pi \left(\frac{\text{RS}}{1 - n + n\Phi_j} \right) \quad (14)$$

where Φ_i and Φ_j are isotopic fractionation factors for isotopically exchangeable hydrogen sites in the transition state (TS) and reactant state (RS) respectively and k'_o is the rate constant in pure H_2O . If the reaction proceeds through a single transition state [37], then



Scheme 7. Hypothesis for the mechanism and oxidative degradation pathway of indigo dyes.

enthalpy of activation suggest that the transition state is highly solvated, while the high negative entropy of activation indicates the formation of rigid associated transition states. The values of ΔG^\ddagger are almost the same in the cases of azobenzene and indigo, suggesting that the oxidative degradation process proceeds by a common mechanism.

It was felt reasonable to compare the oxidation process of azobenzene and indigo in the absence of iron catalyst under identical set of experimental conditions in order to evaluate the catalytic efficiency of iron-catalyst. For this reason, the reactions were studied at different temperatures (333–353 K) in the absence of iron catalyst. From the plots of $\log k'$ vs $1/T$ (Fig. 6. $R^2 > 0.9900$), we evaluated the activation parameters for the uncatalyzed reactions (Table 6). The similar reactivity trend was also observed for the uncatalyzed reactions in which reaction rate of azobenzene is greater than indigo. However, the iron complex catalyzed reactions were found to be 15–20 times faster. Thus the observed rates in the presence of catalyst **5** justify the need of catalyst for facile oxidative degradation of dyes by the chosen Br_3^- oxidant in alkaline medium. The activation parameters evaluated for the catalyzed and uncatalyzed reactions explain the catalytic effect on the reaction.

The catalyst forms transient complex (X) with dyes, which enhances the oxidation process of dyes than without iron catalyst. Further, the reaction rates with respect to azobenzene oxidation are higher than that of indigo oxidation. This can be attributed to the fact that the $-\text{N}=\text{N}-$ bond in azobenzene is electronically rich when compared to $-\text{C}=\text{C}-$ bond in indigo. The catalyst species can be attacks electron rich $-\text{N}=\text{N}-$ bond easier and faster when compared to $-\text{C}=\text{C}-$ bond and there by increases the degradation process in azobenzenes.

3.10. Catalytic activity of iron catalyst

The following equation was derived [39] to relate both catalyzed and uncatalyzed reactions:

$$k_1 = k_0 + K_C[\text{catalyst}]^x \quad (16)$$

in which k_1 is the observed pseudo first-order rate constants obtained in the presence of catalyst **5**, k_0 is the pseudo first-order rate constants for the uncatalyzed reactions, K_C is the catalytic constants and x is the order of the reaction with respect to catalyst **5**.

In the present investigations, 'x' values for the standard run were found to be 1 for both azobenzene oxidation and indigo oxidation. Then the value of K_C is calculated using Eq. (16). The values of K_C have been evaluated for each dye at different temperatures (323–353 K) and K_C was found to vary with temperature. Further, plots of $\log K_C$ vs $1/T$ were linear ($R^2 > 0.9881$) and the values of energy of activation and other activation parameters for the catalyst 5 were computed and were summarized in Table 6.

3.11. Reactions with other polymer supported trihalide reagents

The degradation processes were also been carried out with other trihalide reagents, such as Cl_3^- , I_3^- , Br_2Cl^- , and found that the reactions were faster with Cl_3^- and remarkably with interhalogen Br_2Cl^- . The reactivity sequence follows the order: $\text{Cl}_3^- > \text{Br}_2\text{Cl}^- > \text{Br}_3^- > \text{I}_3^-$. This reactivity trend might be attributable to the redox potentials of halogens. The redox potential of F_2 (1.36) is greater than that of Br_2 (1.07) and which is greater than I_2 (0.54). The high reactivity of Br_2Cl^- is due to the presence of weaker $\text{Br}_2\text{--Cl}$ bond compared to $\text{Br}_2\text{--Br}$ bond and hence the Br_2Cl^- undergoes faster dissociation to furnish Br_2 rather than that of Br_3^- .

4. Conclusions

The inexpensive, stable and convenient Fe-terpyridine–pyridine carboxylate catalyst system has been developed for the selective oxidative conversion of hazardous dyes. In general, the protocol allows oxidative conversion of both azo and indigo dyes into useful molecules, such as nitroarenes and anthranilic acids. The detailed catalysis, mechanistic and kinetics studies have been made. Catalyzed oxidative degradation reactions of both the dyes undergo with similar oxidation mechanism and follow the identical kinetic behavior. Catalyzed reactions are found to be 15–20-fold faster than the uncatalyzed reactions. The observed results have been explained by a plausible mechanism and the related identical kinetic model was designed. The present method developed for the degradation of dyes offers many advantages including high conversion, short reaction times and the involvement of non-toxic reagents.

References

- [1] R.J. Chudgar, Azo dyes, in: J.I. Kroschwitz, M.H. Grant (Eds.), *Kirk-Othmer Encyclopaedia of Chemical Technology*, vol. 3, 4th ed., Wiley, New York, 1994, pp. 821–823.

- [2] K.M. Shah, *Handbook of Synthetic Dyes and Pigments*, vol. 1, Mutitech Publishing, Mumbai, 1998.
- [3] C. O'Neill, F.R. Hawkes, D.L. Hawkes, N.D. Lourenco, H.M. Pinheiro, W. Delee, *J. Chem Technol. Biotechnol.* 74 (1999) 1009–1018.
- [4] K. Hunger, *Chimia* 48 (1994) 520; K. Hunger, *Rev. Prog. Color. Relat. Top.* 35 (2005) 76–78.
- [5] C. Lagrasta, I.R. Bellobono, M. Bonardi, *J. Photochem. Photobiol. A* 110 (1997) 201–205.
- [6] C.A.K. Gouvea, F. Wypych, S.G. Moraes, N. Duran, N. Nagata, P.P. Zamora, *Chemosphere* 40 (1999) 433–440.
- [7] B. Neppolian, S. Sakthivel, B. Arabindoo, M. Palanichamy, V. Murugesan, *J. Environ. Sci. Health* 34A (1999) 1829–1834.
- [8] B. Neppolian, H.C. Choi, S. Sakthivel, B. Arabindoo, V. Murugesan, *Chemosphere* 46 (2002) 1173–1181.
- [9] B. Utset, J. Garcia, J. Casado, X. Domenech, J. Peral, *Chemosphere* 41 (2000) 1187–1192.
- [10] J. Oakes, P. Gratton, I. Weil, *J. Chem. Soc., Dalton Trans.* (1997) 3805–3810.
- [11] J. Oakes, G. Welch, P. Gratton, *J. Chem. Soc., Dalton Trans.* (1997) 3811–3815.
- [12] J. Oakes, P. Gratton, *J. Chem. Soc., Perkin Trans. 2* (1998) 2563–2568.
- [13] D.M. Gould, W.P. Griffith, M. Spiro, *J. Mol. Catal. A: Chem.* 175 (2001) 289–291.
- [14] P. Verma, P. Baldrian, F. Nerud, *Chemosphere* 50 (2003) 975–979.
- [15] R. Tosik, S. Wiktorowski, *Ozone: Sci. Eng.* 23 (2001) 295–299.
- [16] N. Chahbane, D.L. Popescu, D.A. Mitchell, A. Chanda, D. Lenoir, A.D. Ryabov, K.W. Schramma, T.J. Collins, *Green Chem.* 9 (2007) 49–57.
- [17] J.K. Joshi, V.R. Patel, K. Patel, *Indian J. Chem. Pharm. Sci.* 69 (2007) 697–702.
- [18] A. Thorarensen, J. Li, B.D. Wakefield, D.L. Romero, K.R. Marotti, M.T. Sweeney, G.E. Zurenko, *Bioorg. Med. Chem. Lett.* 17 (2007) 3113–3116.
- [19] C.H. Vinod Kumar, R.V. Jagadeesh, K.N. Shivananda, Y.S. Sandhya, C.N. Raju, *Ind. Eng. Chem. Res.* 49 (2010) 1550–1560.
- [20] R.V. Jagadeesha, Puttaswamy, *J. Phys. Org. Chem.* 21 (21) (2008) 844–858.
- [21] S.S. Stahl, *Science* 309 (2005) 1824–1826.
- [22] R.V. Jagadeesh, N. Vaz Puttaswamy, N.M.M. Gowda, *AIChE J.* 54 (2008) 756–765.
- [23] J. Tang, P. Gamez, J. Reedijk, *Dalton Trans.* 7 (2007) 4644–4646.
- [24] I.E. Markó, P.R. Giles, M. Tsukazaki, S.M. Brown, C.J. Urch, *Science* 274 (1996) 274–276.
- [25] R.D. Arasasingham, G.X. He, T.C. Bruice, *Am. Chem. Soc.* 115 (1993) 7985–7991.
- [26] G. Georges, *Ind. Eng. Chem. Res.* 44 (2005) 8468–8472.
- [27] H. Philip, *Chem. Soc. Rev.* 26 (1997) 417–424.
- [28] S. Kajigaeshi, T. Kakinami, *Ind. Chem. Lib.* 7 (1995) 29–48.
- [29] G. Kar, A.K. Saikia, U. Bora, S.K. Dehury, M.K. Chaudhuri, *Tetrahedron Lett.* 44 (2003) 4503–4505.
- [30] J. Berthelot, Y. Benammar, C. Lange, *Tetrahedron Lett.* 32 (1991) 4135–4136.
- [31] A.E. Bradfield, B. Jones, K.J. Orton, *J. Chem. Soc.* (1929) 2810–2814.
- [32] M. Ardon, *J. Chem. Soc.* (1957) 1811–1815.
- [33] E.S. Amis, G. Jaffe, *J. Chem. Phys.* 10 (1942) 598–601.
- [34] C.J. Collins, N.S. Bowman, *Isotope Effects in Chemical Reactions*, Van Nostrand Reinhold, New York, 1970, pp. 267.
- [35] W.J. Albery, M.H. Devics, *J. Chem. Soc. Faraday Trans.* 68 (1972) 167–190.
- [36] G. Gopalakrishnan, J.L. Hogg, *J. Org. Chem.* 50 (1985) 1206–1209.
- [37] N.S. Isaacs, *Physical Organic Chemistry*, Wiley, New York, 1987, pp. 275.
- [38] O. Exner, *Chem. Commun.* (2000) 1655–1658, and references therein.
- [39] E.A. Moelwyn, Hughes, *Kinetics of Reaction in Solutions*, Oxford University Press, London, 1947, pp. 297–299.